Available online at www.sciencedirect.com
SCIENCE DIRECT®
Journal of Catalysis 224 (2004) 69–79
JOURNAL OF CATALYSIS
www.elsevier.com/locate/jcat

Surface modification of fluorinated aluminas: Application of solid state NMR spectroscopy to the study of acidity and surface structure

Peter J. Chupas [1] and Clare P. Grey *

Department of Chemistry, State University of New York at Stony Brook, Stony Brook, NY 11794-3400, USA

Received 2 December 2003; revised 6 February 2004; accepted 11 February 2004

Abstract

Solid-state NMR methods have been used to determine the mechanism for the fluorination reaction of $CHClF_2$ on alumina. The initial stages of fluorination lead to the formation of terminal F–Al groups (i.e., fluorine bound through a single bond to an aluminum atom), which is consistent with a recent XPS report [O. Boese, W.E.S. Unger, E. Kemnitz, S.L.M. Schroeder, Phys. Chem. Chem. Phys. 4 (2002) 2824]. ^{27}Al NMR indicates that five-coordinate aluminum sites are initially consumed during the fluorination reaction, suggesting that the five-coordinate aluminum species are predominately localized near the surface of the high surface area ($\sim$ 3–5 nm) alumina particles. The sorption of basic phosphines as probe molecules for acid sites, coupled with ^{31}P NMR, was used to follow the changes in acidity after fluorination of the surface. The untreated alumina samples do not contain Brønsted acid sites, partial fluorination of the surface leading to their creation. In contrast, the Lewis acid sites, initially present on the untreated alumina, decrease in concentration on fluorination. Continued fluorination of the surface eventually leads to the destruction of the Brønsted acid sites, some Lewis acid sites remaining but in lower concentrations than on the initial untreated alumina.

Keywords: NMR; Fluorinated; Alumina; Acid

1. Introduction

Surface modification is often used to tune reactivity in the field of heterogeneous catalysis, and it is common for solid catalysts to be pretreated or chemically modified before the desired reactivity is observed. For example, the addition of chlorine and/or fluorine to the surface of alumina has been shown to modify acidity and, subsequently, activity for acid-catalyzed F/Cl halogen exchange [1,2], alkylation [3,4], isomerization [5,6], and cracking reactions [7]. Recently, halogenated aluminas, both chlorinated and fluorinated, have attracted considerable attention for use as solid acid catalysts [1–7]. One potential drawback to these catalysts is the observed decrease in activity with time on stream. The drastic changes in activity that result from fluorine addition are believed to be associated with distinct structural changes, and it is these changes that have yet to be fully elucidated.

The surface structure of catalytic aluminas should first be considered to monitor further chemical modification of surface structure. The common catalytic aluminas, γ-Al_2O_3 and η-Al_2O_3, are nonstoichiometric in that they contain significant concentrations of protons. The surfaces of these catalytic transition aluminas are covered with hydroxyl groups bound to sites of various geometries. Knozinger and Ratnasamy's review on the surface structure of aluminas described five types of surface sites [8]. The μ_1-OH groups are referred to as type Ia and Ib and are bound to single tetrahedral and octahedral aluminum atoms, respectively. Two types of μ_2-OH groups, one bound to a tetrahedral and octahedral aluminum (IIa) and the other to two octahedral aluminum atoms (IIb) and a μ_3-OH group bound to three octahedral aluminum atoms (IIIb) were also discussed [8]. Other types of surface hydroxyls may also result from the presence of five-coordinate aluminum species, such as a μ_2-OH group bound to a five- and six-coordinate aluminum site.

The different surface hydroxyls have inherently different acidic properties. For example, μ_2-OH species show Brønsted acid properties while μ_1-OH species do not [8]. Fluorination can significantly modify the acid properties of

* Corresponding author. Fax: (631)632-5731.
E-mail address: cgrey@mail.chem.sunysb.edu (C.P. Grey).
[1] Current address: Materials Science Division, Argonne National Laboratory, Argonne, IL 60439, USA.

0021-9517/$ – see front matter
doi:10.1016/j.jcat.2004.02.013

oxide catalysts and, for alumina, can lead to a strengthening of the acid sites [1–7]. Several techniques have been employed to study the effects of the fluorination of aluminum oxide, including NMR [9–12], XANES (X-ray absorption near-edge spectroscopy) [13], IR [14–17], and X-ray diffraction [9,10,19–21]. There has been considerable discussion in the literature as to the basis of the modification of both Brønsted and Lewis acidity on the surface of alumina. Two conclusions seem to be universal: (1) that stronger Lewis acid sites form as a result of fluorination and (2) that fluorination leads to the formation of Brønsted acid sites on the surface of partially fluorinated alumina.

Previous studies of fluorinated aluminas have employed fluorinating agents such as NH_4F [9,11,12,14,17,18], HF [23], F_2 [21], and $CHClF_2$ [10,13,22]. Our work has, however, shown that the fluorination mechanism depends strongly on the fluorinating agent employed [13]. Acidic protons on the fluorinating agent, and the mode of oxygen removal as either H_2O or CO, for example, may alter the surface structure and acidic properties of the intermediates that are formed. Changing the fluorinating agent may also affect the surface sites that are attacked first during the initial fluorination reactions. This becomes particularly relevant when halocarbons are used as fluorinating agents. For example, $CHClF_2$ and CHF_3 would be expected to attack different surface sites, $CHClF_2$ chemisorbing as a carbocation and CHF_3 adding as a carbanion.

Studies investigating the acidic properties of fluorinated aluminas have coupled the use of probe molecules with IR spectroscopy, allowing the changes to acid properties to be quantified. For example, Peri has demonstrated an increase in the strength of the Lewis acid sites on aluminas fluorinated with NH_4F [14]. In line with this, Scokart et al. have applied IR methods and have concluded that strong Lewis acid sites and stronger Brønsted acid sites form as a result of fluorination of the oxide surface, in aluminas fluorinated with aqueous solutions of NH_4F [17].

A recent report by Boese et al. has investigated the initial stages of the fluorination of γ-Al_2O_3 with $CHClF_2$ using XAES (X-ray excited Auger electron spectroscopy) and XANES [13]. They demonstrated that the surface of the particles is first fluorinated with the formation of singly bound fluorine species (F–Al). This is followed by destruction of the oxide lattice and concurrent formation of strong Lewis acid sites. Lastly, an AlF_3 phase with a high defect concentration is formed. Our previous work, which utilized in situ X-ray diffraction, has also shown that further fluorination of the oxide leads to the formation of an AlF_3 phase that resembles α-AlF_3 but contains significant concentrations of defects [10]. While these analytical methods are able to track the specific structural changes that occur, they do not allow these changes to be directly correlated with the changing nature of the acid sites present on the surface.

Here, we report a single- and double-resonance solid-state NMR study of the structural changes that are associated with the fluorination of the surface of alumina xerogels by the chlorofluorocarbon $CHClF_2$. The basic probe molecule (phenyl dimethylphosphine) is used in conjunction with ^{31}P NMR to quantify the number and types of acid sites. We show that fluorination of the surface leads to the formation of Brønsted acid sites with the concurrent consumption of Lewis acid sites and provide a structural model for the change in the surface structure that is also able to rationalize the observed changes in acidity.

2. Experimental

2.1. Sample preparation

Aluminum-*sec*-tributoxide (99%) and chlorodifluoromethane (HCFC-22) were obtained from Aldrich. The aluminas were prepared as follows: Aluminum-*sec*-tributoxide (ASB) was dissolved in 2-butanol (molar ratio 1:16). While stirring vigorously, 3.5 eq of water per ASB molecule were added dropwise at room temperature. The solution was stirred vigorously for 1 h at room temperature and was then aged for 24 h at 95 °C in a covered glass dish. The resulting gel was subsequently dried at 95 °C for 24 h. The dried material was calcined under nitrogen as follows: 10 °C/min to 400 °C, 400 °C hold for 30 min, followed by rapid cooling to room temperature. This sample, referred to as untreated alumina, is labeled U/Al_2O_3. A dehydrated sample, D/Al_2O_3, was prepared by drying a sample under vacuum to 400 °C at a rate of 2 °C/min and holding at 400 °C for an additional 4 h.

Surface fluorination of the samples was performed in a controlled manner using a vacuum line for low fluorination levels and a reactor tube for higher fluorination levels. All samples were heated and dried under vacuum, from room temperature to 400 °C at a rate of 2 °C/min. 100 Torr of $CHClF_2$ was added to a 162-mL volume vacuum line to which a tube containing a shallow bed of approximately 100 mg of alumina (described above) was attached. After the sample was heated for 2 h at 400 °C, the sample was evacuated for 30 min. This procedure was repeated once for the sample labeled F1/Al_2O_3 and twice for sample F2/Al_2O_3. Sample F1/Al_2O_3 was heated an additional 2.5 h at 400 °C so that both samples received the same overall heat treatment. Sample F3/Al_2O_3 was prepared in a 1/4-in. Inconel reactor, by flowing $CHClF_2$ over the alumina sample at a rate of 40 cc/min. The sample was initially heated to 280 °C under a flow of dry N_2. The flow of $CHClF_2$ was then initiated and continued for a total of 75 min. Gas flow was then switched back to dry nitrogen and the sample was heated to 400 °C for an additional 2 h. Sample surface areas were determined by N_2 physisorption according to the BET method using a Micromeritics ASAP 2010 volumetric sorption analyzer, and the results are given in Table 1. A Leo 1550 field emission gun scanning electron microscope was used to conduct EDS (energy-dispersive X-ray spectroscopy) analysis,

Table 1
Sample composition and surface properties

Sample	Surface area (m^2/g)	% F by mass	# fluorine per surface Al	Lewis acid sites ($mmol/m^2$)	Lewis acid sites (#/surface Al)	Brønsted acid sites ($mmol/m^2$)	Brønsted acid sites (#/surface Al)
D/Al_2O_3	406	0	0	0.001253	0.1258	0	0
$F1/Al_2O_3$	392	6.8	0.91(1.82)[a]	0.000416	0.0417	0.000505	0.0507
$F2/Al_2O_3$	372	10.7	1.52(3.04)	0.000147	0.0148	0.001099	0.1104
$F3/Al_2O_3$	345	20.8	3.19(6.38)	0.000529	0.0531	0.000333	0.0334

[a] Calculated by assuming Al–F terminal groups and (Al–F–Al bridging F atoms).

to determine the fluorine and chlorine contents of the treated samples.

2.2. Phosphine loading

Dimethyl phenylphosphine (Aldrich) was used as the probe molecule for the study of the acidity of the fluorinated alumina samples. The samples were handled under dry N_2 for all manipulations performed after the fluorination procedure. Phosphine loadings were made directly on the samples in the glove box by using a μL syringe with 0.05-μL accuracy. The loading level of phosphine was approximately 0.0018 $mmol/m^2$ for each sample. The samples were immediately sealed in a 4-mm rotor with specially designed airtight spacers. The samples were allowed to equilibrate for 1 h before spectra were acquired.

2.3. NMR

^{19}F MAS NMR experiments were performed with a custom-built 2.0-mm probe, capable of spinning to speeds of 50 kHz, on a Chemagnetics (8.45 T) spectrometer. Fluorine contents of the samples were determined by ^{19}F spin counting using a known mass of aluminum fluoride trihydrate, $AlF_3{\cdot}3H_2O$, as a standard (Table 1). The Hartmann–Hahn condition for the $^{19}F/^{27}Al$ CP (cross polarization) MAS experiments was determined with $AlF_3{\cdot}3H_2O$ and optimized for the so-called fast spinning regime [24], using a radio frequency (rf) field strength for ^{27}Al of approximately 18 kHz. A rotor synchronized contact time of 95 μs was used for MAS frequencies of 42 kHz, with repetition times of 2 s. $^{19}F/^{27}Al$ TRAPDOR (TRAnsfer of Populations in DOuble Resonance) [27] NMR experiments were performed using an ^{27}Al rf field strength of 90 kHz. Chemical shifts are referenced to 1.0 M aqueous aluminum sulfate and hexafluorobenzene as external standards at 0.0 and −163.0 ppm, respectively.

^{27}Al MAS NMR and $^{19}F/^{27}Al$ HETCOR (HETeronuclear CORrelation) NMR experiments were performed with a double-tuned 2.5-mm Bruker probe, on a Bruker Avance 700 (17.1 T) spectrometer. Small ^{27}Al flip angles were used ($< 15°$) to ensure uniform excitation of all spins. CP was used to transfer magnetization from ^{19}F to ^{27}Al for the $^{19}F/^{27}Al$ HETCOR experiments. The Hartmann–Hahn condition for the $^{19}F/^{27}Al$ HETCOR experiments was determined with anhydrous aluminum fluoride and optimized as described above. The typical contact time was approximately 100 μs for MAS frequencies of 35 kHz. Repetition times of 4 s were used.

^{1}H-decoupled ^{31}P MAS NMR experiments were performed with a double-tuned 4.0-mm Chemagnetics probe on a CMX-360 spectrometer at operating frequencies of 360.03 for ^{1}H and 145.45 MHz for ^{31}P. Chemical shifts are referenced to tetramethylsilane and 85% H_3PO_4 as external standards at 0.0 ppm. Zirconia rotors capable of spinning 18 kHz were used for all experiments. Samples were moved directly from a dry atmosphere glove box to the NMR probe, where dry nitrogen was used for the purge and spinning gases. $^{19}F/^{31}P$ REDOR (Rotational Echo in DOuble Resonance) experiments were performed using a double-tuned 3.2-mm Chemagnetics probe. REDOR experiments were performed at −120 °C at a spinning rate of 20 kHz, by applying π pulses to the ^{31}P channel using XY-8 phase cycling [26].

3. Results

3.1. Surface areas

The method of fluorination was chosen so as to maintain high surface areas of the fluorinated materials. As the fluorine content increases from 0 to 21% by mass, the surface area decreases from 406 to 345 m^2/g (Table 1). Although this is a measurable decrease in surface area, the overall surface areas remain high, which makes the systems ideal for study by NMR methods.

3.2. Determination of chlorine content

EDS analysis was performed on samples D/Al_2O_3, $F1/Al_2O_3$, $F2/Al_2O_3$, and $F3/Al_2O_3$, to determine if chlorine was present in the treated samples. No chlorine was observed in the samples, while the fluorine contents obtained were similar to those determined from the NMR experiments reported in the next section. The fluorinated samples used in this study were prepared under low-pressure conditions and were heated under vacuum to remove any adsorbed molecular species before examination by NMR. This may result in the complete removal of HCl as a gas-phase byproduct of the fluorination. These results are in agreement

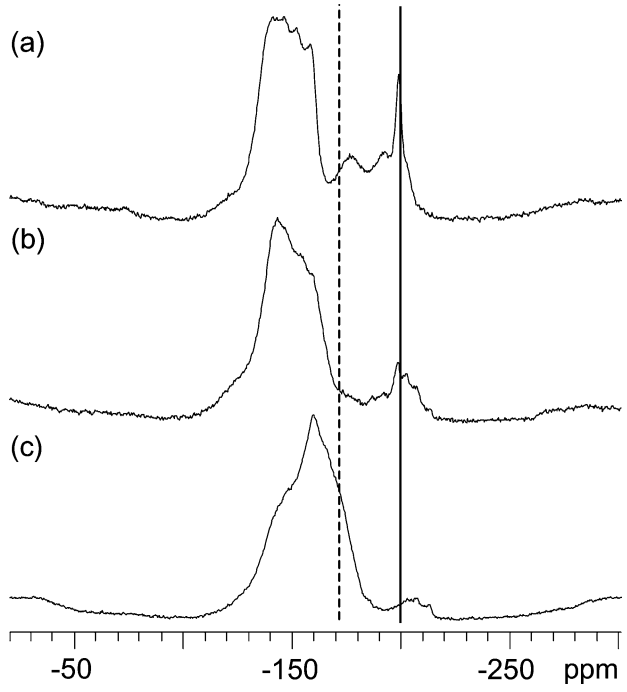

Fig. 1. ^{19}F MAS NMR collected at a spinning speed of 42 kHz for samples (a) F1/Al_2O_3, (b) F2/Al_2O_3, and (c) F3/Al_2O_3. Guidelines are shown at the ^{19}F chemical shift positions of bulk anhydrous aluminum fluoride at −172 ppm (dashed line) and at −200 ppm (solid line; terminal Al–F groups).

with the results of a detailed XPS study by Boese et al., who found no significant difference between surface fluorination with $CHClF_2$ versus CHF_3 [13]. Although they found evidence for very small amounts of chlorine, <1% (mole), in their samples, fluorination was the dominant reaction, with final F contents of between 5 and 14% (mole) being observed [13]. In addition, in situ diffraction studies of the fluorination of alumina with $CHClF_2$ have shown the formation of aluminum fluoride phases [10]. Clearly, fluorination of the surface is a primary result of treatment with $CHClF_2$, which is reasonable considering that the formation of aluminum fluoride is thermodynamically more favorable than aluminum chloride [2].

3.3. ^{19}F and ^{27}Al MAS NMR

The ^{19}F MAS NMR spectra of the fluorinated samples F1/Al_2O_3, F2/Al_2O_3, and F3/Al_2O_3 are shown in Fig. 1a, 1b, and 1c, respectively. The application of very fast spinning MAS (in excess of 40 kHz) at a field of 8.45 T allows the full chemical shift range, which spans approximately 100 ppm, to be collected without any overlap of the isotropic resonances with the sidebands of different resonances. As the fluorination level increases from F1/Al_2O_3 to F3/Al_2O_3, the chemical shifts and relative abundance of the different sites change with a clear trend. For the lowest level fluorinated sample, F1/Al_2O_3, two groups of peaks are observed, one between −110 and −165 ppm and the other, which consists of several overlapping peaks, between −170 and −220 ppm. As the fluorination level increases, the chemical shifts of both groups of resonances shift to more negative frequencies and the relative intensity of the second group of resonances decreases. The group centered between −110 and −165 ppm has chemical shifts consistent with aluminum oxyfluoride environments (i.e., $AlO_{6-x}F_x$, $1 < x < 6$) [27]. Chemical shifts of −180 to −200 ppm have been observed for alkali metal aluminum fluoride salts [28], the fluorine atoms bonded to a single aluminum (F–Al species) showing chemical shifts in the −200 ppm region. Chemical shifts of −180 to −200 ppm have also been observed for tetrahedral aluminum fluoride species in organic salts and as isolated species in zeolites [29,30].

The surface fluorine concentration was determined by spin counting and is given in Table 1 in units of weight percent and fluorine atoms per surface aluminum atom. The latter values were estimated by making use of the numbers previously reported for the concentrations of tetrahedral and octahedral Al atoms on the surface of nano-sized alumina particles, of 2.8 and 4.0 atoms/nm^2, respectively [8]. The numbers in Table 1 were determined by assuming, first, that each F atom is coordinated to a single Al atom (forming a terminal Al–F species) and, second, that each F atom is coordinated to two Al atoms in bridging Al–F–Al linkages. The second value is given in parentheses in Table 1, these two assumptions representing the two extreme situations for the maximum and minimum numbers of F coordinated to the surface Al atoms. At the highest fluorine loadings, a Al:F ratio greater than 1:6 assuming Al–F–Al bridging groups is consistent with the formation of AlF_6 octahedral environments and the fluorination of more than the first layer of Al surface atoms.

The ^{27}Al MAS NMR spectra of the samples U/Al_2O_3, D/Al_2O_3, F1/Al_2O_3, F2/Al_2O_3, and F3/Al_2O_3 are shown in Fig. 2a, 2b, 2c, 2d, and 2e, respectively. The spectra each contain three major groups of resonances, centered at 70, 35, and 10 ppm, which correspond to four-, five-, and six-coordinate aluminum species, respectively. Significant changes are apparent as the fluorination level increases. The most apparent change is in the relative number of five-coordinate aluminum sites, the number of these sites decreasing with fluorination level. This is best illustrated in Fig. 2f, which shows the overlaid ^{27}Al NMR spectra of samples D/Al_2O_3 and F1/Al_2O_3. The six-coordinate resonance shifts to more negative values on fluorination. This, based on our earlier work [32], indicates an increase in the number of octahedral aluminum oxyfluoride groups, $AlO_{6-x}F_x$ and in the value of x. Consistent with this, the resonance at −16 ppm in Fig. 2e is assigned to an AlF_6 group [32]. Thus, the major process that appears to occur during fluorination is the reaction of the coordinatively unsaturated aluminum sites (i.e., five-coordinate sites) to form octahedral aluminum oxy-fluoride species. The resonance due to the four- coordinate Al atoms sharpens on fluorination and

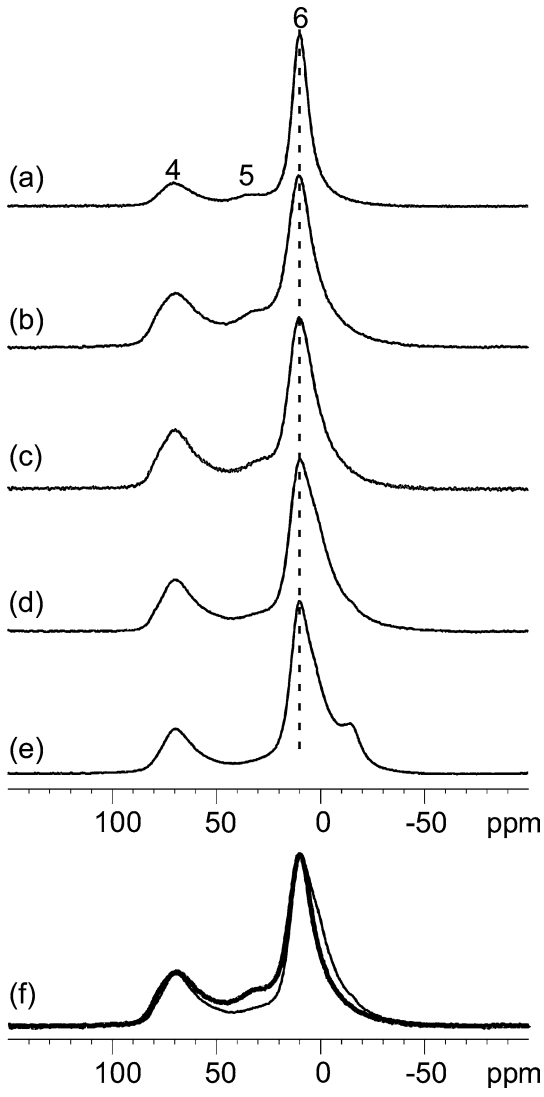

Fig. 2. ^{27}Al MAS NMR collected at a spinning speed of 35 kHz, for samples (a) U/Al_2O_3, (b) D/Al_2O_3, (c) F1/Al_2O_3, (d) F2/Al_2O_3, and (e) F3/Al_2O_3. (f) Overlaid spectra of D/Al_2O_3 (heavy line) and F2/Al_2O_3 (thin line). The guideline is shown at 10 ppm, the chemical shift of a six-coordinate AlO_6 species in γ-Al_2O_3; the assignment of the resonances to different Al coordination numbers are given in (a).

decreases slightly in intensity as some of these sites are also consumed.

3.4. ^{19}F/^{27}Al CP NMR spectroscopy

The cross-polarization (CP) experiment relies on the polarization transfer of net magnetization on one set of nuclei to others in close proximity. The large ^{19}F chemical shift range in the fluorinated samples can be exploited to examine the type of aluminum species associated with the different groups of ^{19}F resonances, as the CP efficiency is very sensitive to the offset frequency of the ^{19}F radio frequency (rf) field, the polarization transfer rate decreasing by an amount $\upsilon_1^2/(\upsilon_1^2+\delta_{\text{off}}^2)$, as the offset frequency (δ_{off}) of the applied rf field strength (υ_1) is increased [31,32]. Here, we use this

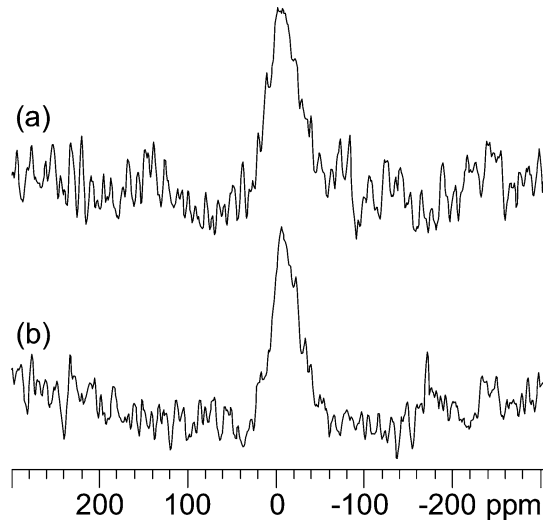

Fig. 3. ^{19}F/^{27}Al CP MAS collected at a spinning speed of 42 kHz, for sample F2/Al_2O_3. The spectra were collected with the ^{19}F offset located at (a) −110 ppm and (b) −220 ppm and a weak ^{19}F rf field strength of 38 kHz.

method to determine whether the majority of fluorine chemical shifts in the range of −180 to −200 ppm are associated with octahedral, five-coordinate, or tetrahedral aluminum species.

The ^{19}F/^{27}Al CP NMR spectra shown in Fig. 3a and 3b were collected with fluorine offsets corresponding to ^{19}F shifts of −110 and −220 ppm, respectively. The only signal observed in both CP spectra has a chemical shift of approximately 0 ppm, which corresponds to octahedral aluminum atoms. There is no indication that either group of ^{19}F resonances are associated with five-coordinate or tetrahedral aluminum species.

3.5. ^{19}F/^{27}Al TRAPDOR NMR

A ^{19}F/^{27}Al TRAPDOR NMR experiment was performed on F1/Al_2O_3 (Fig. 4) to explore differences in the F–Al dipolar couplings, and thus connectivities, of the different fluorine sites. The experiment was performed using fast spinning speeds to obtain the highest resolution possible; the TRAPDOR experiment is still feasible under these conditions due to the small quadrupole coupling constants of the Al atoms [25]. It is clear from the difference spectra that all the fluorine sites are located in close proximity (i.e., directly bound) to aluminum atoms. The resonances between −180 and −220 ppm show a noticeably smaller TRAPDOR fraction than the other resonances at higher frequencies. This is consistent with their assignment to terminal fluorine species bound to a single aluminum atom since they experience an overall smaller F–Al dipolar coupling than fluorine bound to two aluminum atoms in Al–F–Al bridges.

3.6. ^{19}F/^{27}Al HETCOR NMR spectroscopy

The ^{19}F/^{27}Al HETCOR spectrum for sample F2/Al_2O_3 is shown in Fig. 5, and provides a second method for iden-

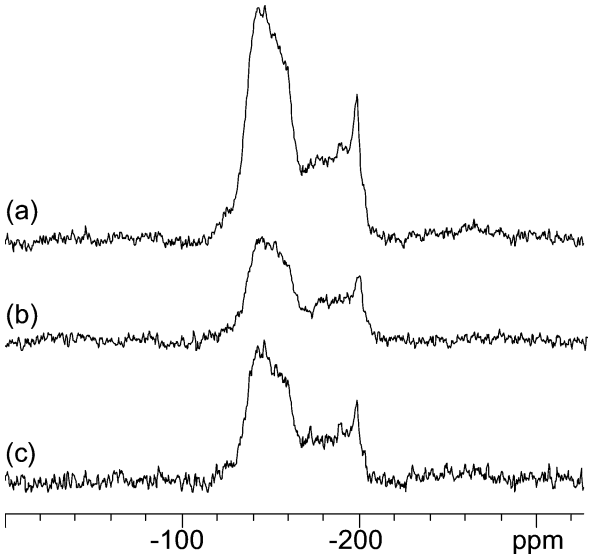

Fig. 4. $^{19}F/^{27}Al$ TRAPDOR NMR of sample F3/Al_2O_3; (a) control, (b) double resonance, and (c) difference, obtained by subtracting the spectrum shown in (b) from that in (a). A spinning speed of 40 kHz was used with 8 rotor periods of irradiation on the ^{27}Al channel.

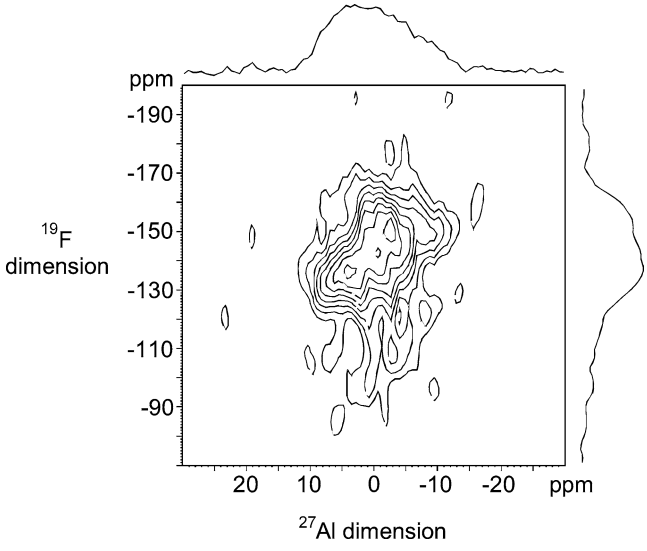

Fig. 5. $^{19}F/^{27}Al$ HETCOR NMR two-dimensional spectra for sample Al_2O_3/F2, collected at a spinning speed of 35 kHz. The ^{27}Al irradiation offset was placed at a shift of 30 ppm.

tifying the Al atoms in close proximity to fluorine. A short contact time ensures that the major peaks in the spectrum correspond to directly bonded Al–F species. The utility of this type of experiment is apparent when a comparison is made between the ^{27}Al dimension and the ^{27}Al one-pulse spectrum of the same sample shown in Fig. 2. The signal from aluminum atoms in close proximity (i.e., directly bonded) to fluorine is selected in the ^{27}Al dimension. The projection of the ^{27}Al dimension is rather featureless, indicating a distribution of sites. The resonances due to these sites are more dispersed in the two-dimensional spectra, and the ^{19}F chemical shift due to each site can now be directly extracted. As the ^{19}F chemical shift moves from −120 to −170 ppm, the chemical shifts of the bonded ^{27}Al species move from 0 to −10 ppm. This shift correlates to an increasing fluorination level (i.e., x increasing in $AlO_{6-x}F_x$), again consistent with our earlier work [32]. The ^{19}F signal at −200 ppm (not shown) overlaps with the sideband of the resonance centered at −150 ppm, and it is therefore impossible to say with certainty which aluminum species it is connected to.

3.7. ^{27}Al MQ-MAS NMR spectroscopy

The ^{27}Al MQ-MAS spectra collected at 16.3 T, for the D/Al_2O_3 and all the fluorinated samples, are shown in Fig. 6. There are two major clusters of resonances. The isotropic chemical shift of the four-coordinate tetrahedral Al site is centered at 70 ppm, while that for the six-coordinate octahedral site is centered near 10 ppm, in the anisotropic dimension. As the fluorination process proceeds, an upfield shoulder of the six-coordinate peak, due to the oxyfluoride sites, emerges. These sites are particularly noticeable in 6c and the AlF_6^{3-} resonance is clearly seen in 6d. Two different four-coordinate sites are also resolved in the spectra shown in Fig. 6a, 6b, and 6c, at approximately 70 and 75 ppm (in the anisotropic dimension of the MQ-MAS spectra). The 75 ppm resonance is no longer present in the MQ-MAS spectrum of the most highly fluorinated sample and only a single, broad four-coordinate site is visible at lower frequencies. The four-coordinate sites most affected by fluorination are likely either localized near the surface and, therefore, consumed first, or are connected to a five-coordinate site and thus could be indirectly perturbed by the fluorination of that species. The five-coordinate sites, just visible above the noise in Fig. 6a, are consumed during fluorination. This is seen more clearly in higher signal-to-noise MQ-MAS spectra acquired with a larger volume 4-mm probe.

3.8. ^{31}P MAS NMR

The variable temperature ^1H decoupled ^{31}P MAS NMR spectra of the alumina and fluorinated alumina samples loaded with dimethyl phenylphosphine (DMPP) are shown in Fig. 7. Three discrete sites are observed for the spectra acquired at −150 °C, which are assigned to physisorbed phosphine molecules (approximately −45 ppm), phosphines bound to Lewis acid sites (i.e., coordinatively-unsaturated aluminum; −35 ppm) and protonated phosphine ions bound directly to the conjugate bases of the Brønsted acid (surface) sites (approximately 0 ppm) [23,27]. At room temperature, molecular exchange of the phosphine molecules occurs, particularly between the Lewis acid site-bound phosphines and the physisorbed molecules, but this exchange can be frozen out by cooling to −150 °C. This exchange results in inaccurate measurements of the ^{31}P chemical shift and relative number of sites at room temperature and the concentrations

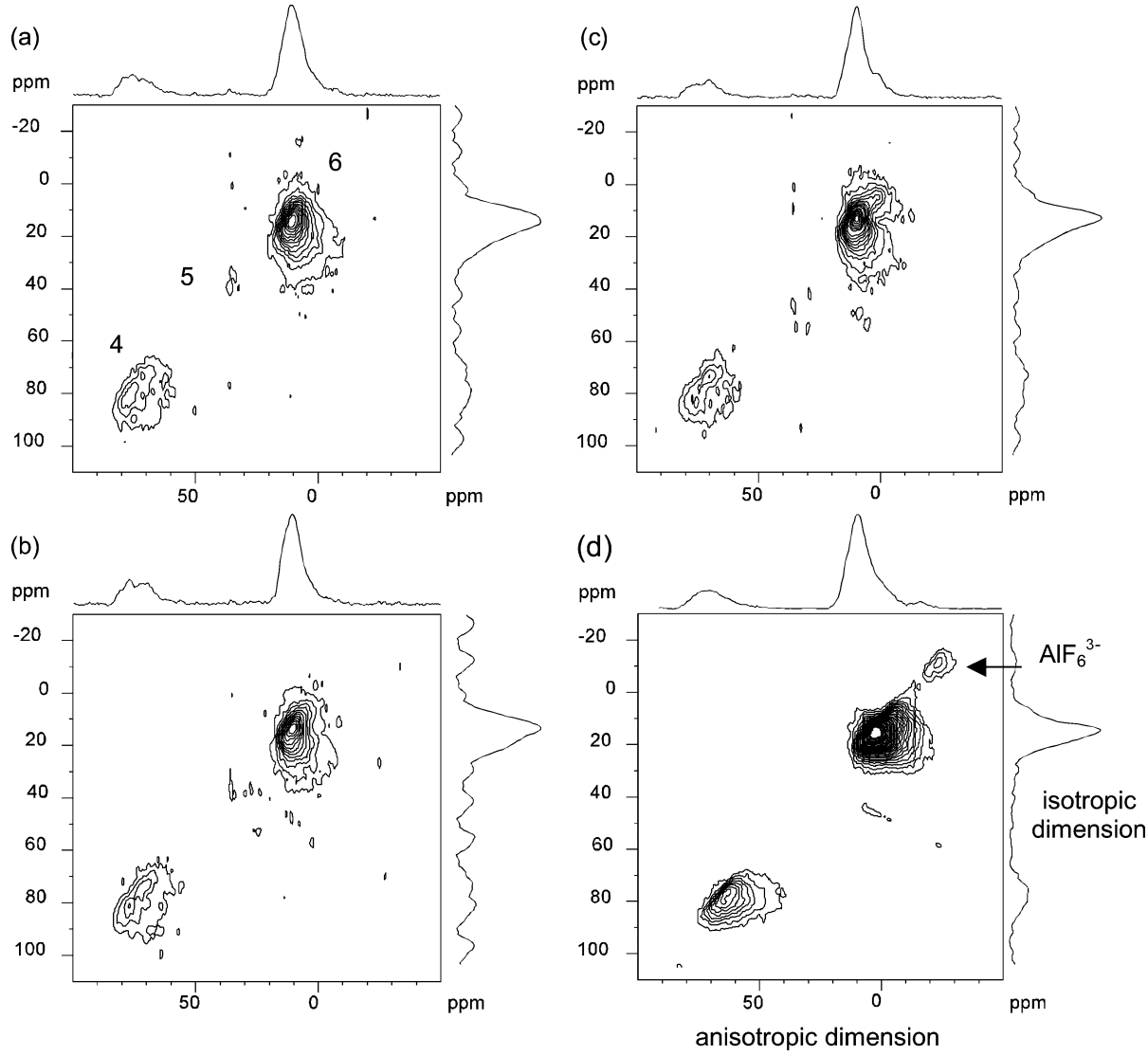

Fig. 6. ^{27}Al MQ-MAS NMR collected at a spinning speed of 35 kHz on a 16.3 T spectrometer, for samples (a) D/Al_2O_3, (b) F1/Al_2O_3, (c) F2/Al_2O_3, and (d) F3/Al_2O_3. The assignments of the resonances to different Al coordination numbers are shown in (a) and the AlF_6^{3-} species is marked in (d).

of the different sites given in Table 1 were obtained from the low-temperature NMR data.

Differences are apparent between the untreated alumina and fluorinated samples. The untreated alumina does not contain any strong Brønsted acid sites, as no resonance is observed in the 0 ppm region. As the surface fluorination proceeds, the concentration of Lewis acid sites decreases from the level originally observed on the untreated sample. In contrast, the concentration of Brønsted acid sites grows, from F1/Al_2O_3 to F2/Al_2O_3, but drops noticeably for the highest F content sample.

3.9. $^{19}F/^{31}P$ REDOR NMR

We have used the REDOR NMR experiment (Fig. 8) to probe the proximity of fluorine on the catalyst surface to the phosphorus atom on the adsorbed phosphine for F1/Al_2O_3 loaded with DMPP. A noticeable change in the ^{19}F chemical shifts is apparent on sorbing the phosphine (Fig. 1a), the two major groups of resonances shifting to lower frequencies to −120 to −160 and −160 to −200 ppm. The larger change in chemical shift seen for the terminal Al–F groups (−160 to −200 ppm) is reasonable since these species might be expected to interact more strongly with the phosphine molecules than the more buried Al–F–Al species. This change in chemical shift has also been observed for samples that have been allowed to hydrate and might explain why samples fluorinated under hydrous environments by other workers have shown very different ^{19}F NMR spectra [11,12].

Two discrete groups of fluorine resonances from fluorine atoms near phosphorus, one centered at −135 ppm and the other at −180 ppm, are seen in the difference spectrum. The relative concentration of the terminal F atoms (−180 ppm) is increased in the difference spectrum relative to the control, again consistent with the presence of these groups on the surface. Sample F1/Al_2O_3 contains two types of acid sites,

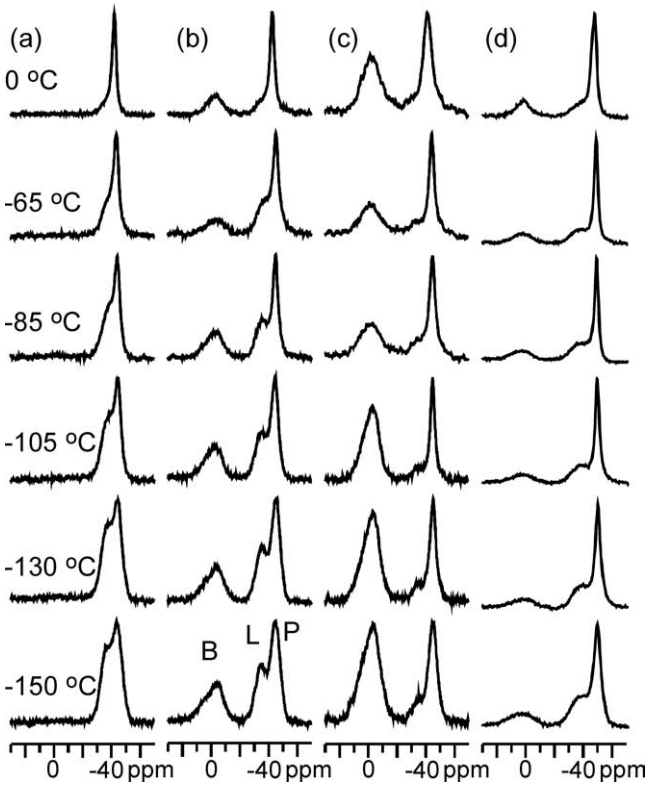

Fig. 7. Variable temperature ^{1}H decoupled ^{31}P NMR spectra of dimethylphenylphosphine-loaded (a) D/Al_2O_3, (b) F1/Al_2O_3, (c) F2/Al_2O_3, and (d) F3/Al_2O_3. ^{31}P resonances corresponding to coordination to the Brønsted (B) and Lewis (L) and the physisorbed molecules are marked in the low-temperature spectrum of (b).

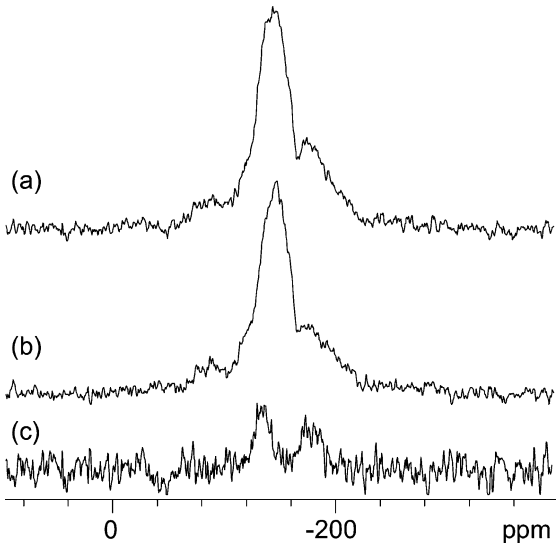

Fig. 8. ^{31}P/^{19}F REDOR NMR of sample F2/Al_2O_3 loaded with dimethylphenylphosphine; (a) control, (b) double resonance, and (c) difference (×2). A 34 rotor period dephasing time was used with XY-8 phase cycling.

which might be expected to be located near different fluorine species. However, Brønsted acid sites are created on fluorination, while the Lewis acid sites are partially destroyed, suggesting that these two F sites may both be associated with the Brønsted acid site.

4. Discussion

Sol–gel-derived aluminas were used in this study for several reasons. First, the synthesis of high surface area materials is relatively straightforward with alkoxide precursors. High surface areas (>300 m^2/g) are clearly advantageous in the application of NMR, an inherently insensitive technique, to the study of surface structure. Second, these aluminas contain few chemical impurities relative to commercial alumina catalyst supports. Since we are studying subtle structural features on the surface of the aluminas, we wanted to minimize the potential of contaminate species.

The phase stability of aluminas prepared using the aluminum alkoxide route has been examined by Wang et al., as a function of temperature [33]. Their work has shown that samples calcined at 400 °C predominately contain the γ-Al_2O_3 phase [33]. The ^{27}Al MAS NMR spectrum of D/Al_2O_3 shows an intensity ratio of approximately 1 to 2 for the tetrahedral to octahedral aluminum sites, in line with the ratios expected for γ-Al_2O_3 [10]. All our samples were dehydrated to 400 °C prior to fluorination; thus, the observation of a phase with regions that are locally similar to γ-Al_2O_3 is not too surprising. Note that the presence of four-coordinate aluminum species is strong evidence for the presence of a spinel-related phase (i.e., a γ or γ' alumina): All the other transition aluminas such as boehmite contain six-coordinated aluminum sites only. The small differences between the ^{27}Al MAS NMR of U/Al_2O_3 and D/Al_2O_3 primarily arise from the loss of some of the residual hydroxyl groups following dehydration under vacuum, which will result in an increase in the number of coordinatively unsaturated aluminum atoms on the surface. The presence of high concentrations of five-coordinate aluminum is a direct consequence of the increased number of defects caused by the high surface area of the materials used in this study and from the disorder that results from the synthesis method used to prepare the materials.

There have been many detailed studies of fluorinated aluminas, which have used different fluorinating agents and/or conditions; thus, the local structures are unlikely to be identical for all procedures. In particular, the mechanism of fluorination of the surface of aluminas is dependent in part on the fluorinating agent and conditions used [2–14]. This is particularly evident when we consider the use of NH_4F as a fluorinating agent. Here, several reports indicate NH_4AlF_4 phase formation [9], which obviously has no role in the fluorination mechanism when halocarbons are used. Thus, in the subsequent discussion of the mechanism of fluorination, we pay particular attention to those studies using halocarbons.

The very fast spinning ^{19}F MAS NMR spectra clearly indicate the presence of two major groups of resonances.

The resonances in the range from −110 to −165 ppm are consistent with octahedral aluminum oxyfluoride environments [32]. The observation of these resonances and their assignments are consistent with other NMR studies. An additional group of resonances between −180 and −220 ppm has not previously been observed on fluorinated aluminas. We assign the majority of these peaks to terminal fluorine species (i.e., fluorine bound to a single aluminum atom) bonded to an octahedral aluminum atom. The chemical shift range of these species, however, is consistent with both tetrahedral and octahedral aluminum fluoride species, with terminal F–Al linkages. Terminal Al_{IV}–F species are not consistent with the $^{19}F/^{27}Al$ CP results. The presence of terminal fluorine species has been clearly observed in fluorination procedures using $CHClF_2$ by Boese et al. using XAES and XANES [13], but these methods were not able to distinguish between four- and six-coordinate species. There are several potential explanations as to why these types of terminal groups have not been previously observed with NMR spectroscopy. Most earlier NMR studies have utilized NH_4F in aqueous solutions to fluorinate the surface and the presence of moisture and the use of fluoride salts may not lead to stable terminal F–Al species. Additionally, overlap with the spinning sidebands of the more intense resonance at lower frequencies may have concealed the resonances of the terminal fluorine species in these earlier studies.

The ^{27}Al MAS and MQMAS NMR spectra provide insight as to which aluminum species are consumed during the initial fluorination reaction. It is apparent from the ^{27}Al MAS NMR spectra that the number of five-coordinate Al decreases during the fluorination process. As these five-coordinate and (higher frequency) four-coordinate species (seen by MQMAS) are consumed, octahedral aluminum oxyfluoride species are formed. The preference for the attack of the five-coordinate sites during the initial stages of fluorination is most likely thermodynamic in nature. Five-coordinate aluminum species are predominately observed in aluminas that have been synthesized through low-temperature procedures, which are capable of trapping metastable five-coordinate Al species. Since the five-coordinate sites are consumed during the first stages of fluorination, this suggests that these species are localized on the surface of the nano-sized (∼5 nm) particles. The ^{27}Al NMR of the dehydrated as-prepared material (D-Al_2O_3) suggests that the γ-Al_2O_3 structure, which is composed of a cubic closed packed array of oxygen atoms with aluminum occupying 8/9 of the octahedral sites and 4/9 of the tetrahedral sites, is a reasonable model of the structure of the particles. The five-coordinate aluminum atoms are most likely located near the surface of such small particles due to surface relaxation and termination effects and are thus more readily fluorinated.

The variable temperature ^{31}P NMR of the adsorbed phosphines clearly indicates the importance of making quantitative measurements at low temperatures to freeze out any molecular exchange processes on the surface. Many previous studies have utilized phosphines as probe molecules, though several have not paid particular attention to the possibility of site exchange at ambient temperatures. In these systems, the motion is not frozen out of the NMR time scale until approximately −80 °C, allowing accurate concentrations of the number of acid sites to be determined. From the quantification of the −150 °C, ^{31}P MAS NMR spectra it is clear that the number of Lewis acid sites decreases on fluorination (Table 1). This is consistent with the increase in the average coordination number of aluminum on the surface as fluorine replaces oxygen. The measured Lewis acidity increases slightly from D/Al_2O_3 to F3/Al_2O_3 as evidenced by the slight downfield shift in ^{31}P chemical shift from −39 to −35 ppm. This may be due to one of several reasons: first, nucleation of a new aluminum fluoride/hydroxyfluoride phase or reaction with a tetrahedral Al atom may open up additional coordinatively unsaturated aluminum centers. Second, fluorination of nearby Al may increase acidity due to inductive effects. The ^{31}P MAS NMR also clearly indicated the formation of Brønsted acid sites from D/Al_2O to F2/Al_2O_3, but these sites are consumed as the fluorine to surface aluminum ratio approaches 3.0 in sample F3/Al_2O_3.

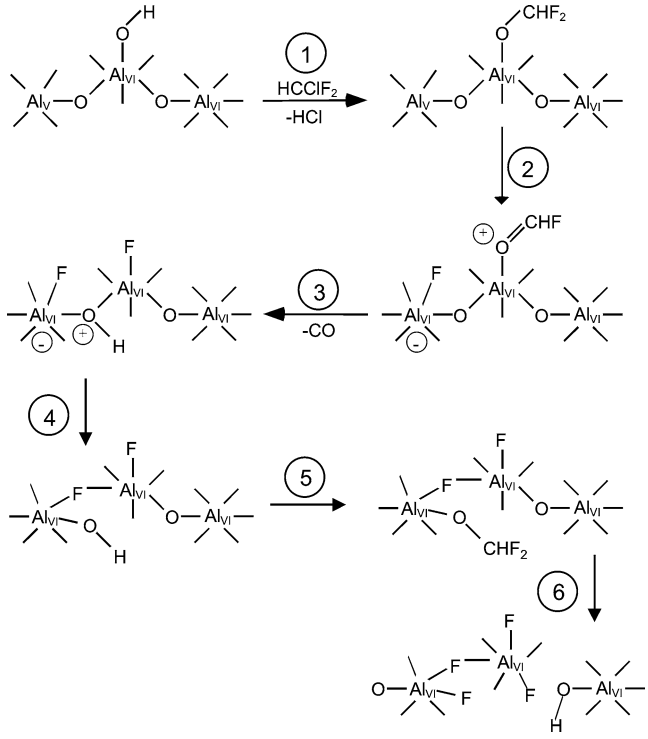

Fig. 9. Diagram of proposed reaction pathway for the first states of fluorination.

Based on the results of this NMR study, we can propose a mechanism for the first stages of fluorination of the surface of alumina with $CHClF_2$ (Fig. 9). The first step involves the chemisorption of a $CHClF_2$ molecule to the surface. Since the relative bond strengths are C–Cl < C–H < C–F, this is likely to occur via C–Cl bond breaking and carbocation formation [34]. The terminal μ_1-OH (Al–OH) groups are stronger nucleophiles than μ_2-OH (Al–O(H)–Al) groups,

for example, and can attack the $CHClF_2$ molecules forming bound methoxy species, $F_2HC–O–Al$ (step 1 in the scheme shown in Fig. 9). The released chloride ions will combine with the proton of the μ_1-OH group, forming HCl, which will be removed as a gaseous by-product. The formation of these types of methoxy species formed through C–Cl bond cleavage has been directly observed for the adsorption of CH_3Cl to alumina, where the presence of hydroxyl groups was found to be essential for the disassociative chemisorption of chloroalkanes [35].

Following chemisorption and formation of the methoxy species, the subsequent steps most likely occur through intermediates with only a transient existence. The fluorine and hydrogen atoms from the methoxy ($–O–CHF_2$) group molecule must clearly react with the surface, as HF will not be desorbed from the surface at the temperature of the fluorination reactions. Five-coordinate, unsaturated sites nearby the methoxy group will be readily fluorinated to form octahedral environments (step 2), leading to an increase in the average coordination environment on the surface, and the conversion of five-coordinate to octahedral environments.

The carbon from the originally chemisorbed $CHClF_2$ molecule is removed from the surface as a carbon monoxide molecule (step 3), the oxygen coming from the initial methoxy bridge. Desorption of CO versus CO_2 was observed in our earlier GC studies [10] and is consistent with the fluorination agent used in this study. $CHClF_2$ would not be expected to undergo any oxidation or reduction reactions following reaction with the alumina surface and must, therefore, be desorbed as CO. CO_2 can, however, be formed as the product of the disproportionation of CO. The desorption of the CO molecule must occur with the simultaneous attack of the Al atom by fluorine so that no unstable three-coordinate aluminum site are formed. The formation of a terminal F–Al group is consistent with the work of Boese et al. who investigated fluorination with the same halocarbon, $CHClF_2$ [13].

Charge balance is maintained, following CO loss, by the protonation of a bridging oxygen species to a form Brønsted acid sites. This process was followed in the ^{31}P NMR spectra, the untreated alumina showing no evidence of the Brønsted acidity increasing steadily on fluorination as the Lewis acidity decreased and the lower coordinate sites were consumed. Reaction of a terminal Al–F group with the nearby Al atom results in the formation of a Al–F–Al linkage, a new μ_1-OH group, and the consumption of the Brønsted acid site. The new μ_1-OH group can then react further with another $CHClF_2$ molecule. Once all the unsaturated sites have been fluorinated, the reaction must then proceed by cleavage of Al–O–Al bonds connecting nearby surface sites (reactions 5 and 6) or an Al–O bond of the μ_1-OH group. These reactions no longer produce Brønsted acid sites.

It is useful to consider the differences between fluorination with halocarbons and aqueous methods. Several workers have investigated the structural changes associated with aqueous impregnation of aluminas with NH_4F. For example, DeCanio et al. have used ^{27}Al NMR to identify different aluminum hydroxyfluoride environments [9] and Fischer et al. have used ^{19}F NMR to distinguish different types of surface Al sites, based on their fluoride substitution levels [11]. In both studies there was no evidence for terminal Al–F groups, suggesting that the use of aqueous methods can modify the fluorination pathway, and either do not lead to the formation of the more labile terminal Al–F species, or if they are formed, they then react further under these conditions to form Al–OH or Al–F–Al groups. DeCanio et al. have shown that high levels of NH_4F also lead to the dissolution of aluminum species and the formation of NH_4AlF_4 salts on the surface, which decompose into β-AlF_3 [9]. This is in marked contrast to the gas-phase reaction of halocarbons with the surface of aluminas, where terminal Al–F groups are clearly observed. Further evidence for the formation of terminal Al–F species in nonaqueous fluorinations was provided by Krahl et al., who have used halocarbons in the fluorination of $AlCl_3$ and have identified terminal Al–F species in the products [36]. Further fluorination with HCF_2Cl leads to the condensation of the terminal groups, and eventually the formation of α-AlF_3, rather than β-AlF_3, albeit with a high concentration of defects [10].

5. Conclusion

The combination of single- and double-resonance solid-state NMR and the use of basic probe molecules have been used to examine the mechanism of fluorination of alumina using $CHClF_2$ as the fluorinating agent. Our study clearly supports a mechanism that occurs in the following steps:

(1) the $CHClF_2$ molecule reacts with a μ_1-OH group with the formation of HCl,
(2) the five-coordinate aluminum sites and Lewis acid sites are consumed, resulting in the formation of Brønsted acid sites and terminal Al–F groups,
(3) condensation of Al–F groups, which results in Al–F–Al linkages, the consumption of the Brønsted acid sites, and the formation of additional μ_1-OH groups, and
(4) the reaction of the newly formed μ_1-OH groups with more $CHClF_2$ molecules and a repeat of steps (2)–(3).

Once the unsaturated Al sites are fluorinated, no new Brønsted acid sites can be created, but fluorination can still continue by cleaving Al–O–Al bonds. The model is consistent with the ^{27}Al and ^{19}F NMR studies of the changing surface structure and the ^{31}P NMR spectra of the sorbed basic phosphines. Whereas no Brønsted acidity is observed in the untreated alumina, strong Brønsted acid sites form during the initial stages of fluorination, which then disappear as the surface is fully fluorinated and the five-coordinated Al sites are consumed.

Controlling the acid properties of alumina requires the development of mechanisms for the modification of its surface. The fluorination mechanism proposed in this work repre-

sents the first step toward the rational control of the acidity of fluorinated aluminas. An understanding of and ability to control acidity may eventually allow acid properties to be tailored to catalyze specific reactions.

Acknowledgments

Martine Ziliox is thanked for her assistance in collection of the high-field NMR data. Financial support from the Basic Energy Sciences program of the Department of Energy is gratefully acknowledged (DEFG0296ER14681).

References

[1] L.E. Manzer, Science 249 (1990) 31;
L.E. Manzer, V.N.M. Rao, Adv. Catal. 39 (1993) 329.
[2] E. Kemnitz, D.-H. Menz, Prog. Solid State Chem. 26 (1998) 97.
[3] L.M. Rodriguez, J. Alcaraz, M. Hernandez, Y. Ben Taarit, M. Vrinat, Appl. Catal. A 169 (1998) 15.
[4] L.M. Rodriguez, J. Alcaraz, M. Hernandez, M. Dufaux, Y. Ben Taarit, M. Vrinat, Appl. Catal. A 189 (1998) 53.
[5] Z. Cheng, V. Ponec, J. Catal. 148 (1994) 607.
[6] R. Covini, V. Fattore, N. Giordano, J. Catal. 7 (1967) 126.
[7] G.B. McVicker, C.J. Kim, J.J. Eggert, J. Catal. 80 (1983) 315.
[8] H. Knözinger, P. Ratnasamy, Catal. Rev.-Sci. Eng. 17 (1978) 31.
[9] E.C. DeCanio, J.W. Bruno, V.P. Nero, J.C. Edwards, J. Catal. 140 (1993) 84.
[10] P.J. Chupas, M.F. Ciraolo, J.C. Hanson, C.P. Grey, J. Am. Chem. Soc. 123 (2001) 1694.
[11] L. Fischer, V. Harle, S. Kastelan, J.B. d'Espinose de la Caillerie, Solid State NMR 16 (2000) 85.
[12] W. Zhang, M. Sun, R. Prins, J. Phys. Chem. B 106 (2002) 11805.
[13] O. Boese, W.E.S. Unger, E. Kemnitz, S.L.M. Schroeder, Phys. Chem. Chem. Phys. 4 (2002) 2824.
[14] J.B. Peri, J. Phys. Chem. 72 (1968) 2917.
[15] Q. Dai, G.N. Robinson, A. Freedman, J. Phys. Chem. B 101 (1997) 4940.
[16] S.S. Deshmukh, V.I. Kovalchuk, V.Y. Borovkov, J.L. d'Itri, J. Phys. Chem. B 104 (2000) 1277.
[17] P.O. Scokart, S.A. Selim, J.P. Damon, P.G. Rouxhet, J. Colloid Interface Sci. 70 (1979) 209.
[18] E.R.A. Matulewicz, F.P.J.M. Kerkoff, J.A. Moulin, H.J. Reitsma, J. Colloid Interface Sci. 77 (1980) 110.
[19] A. Hess, E. Kemnitz, A. Lippitz, W.E.S. Unge, D.H. Menz, J. Catal. 148 (1994) 270.
[20] A. Hess, E. Kemnitz, J. Catal. 149 (1994) 449.
[21] J.M. Saniger, N.A. Sanchez, J.O. Flores, J. Fluorine Chem. 88 (1998) 117.
[22] R.I. Hedge, M.A. Barteau, J. Catal. 120 (1989) 387.
[23] J.H. Lunsford, W.P. Rothwell, W. Shen, J. Am. Chem. Soc. 107 (1985) 1540.
[24] A.J. Vega, Solid State Nucl. Magn. Res. 1 (1992) 17.
[25] C.P. Grey, A.J. Vega, J. Am. Chem. Soc. 117 (1995) 8232.
[26] T. Gullion, D.B. Baker, M.S. Conradi, J. Magn. Res. 89 (1990) 479.
[27] P.J. Chupas, D.R. Corbin, V.N.M. Rao, J.C. Hanson, C.P. Grey, J. Phys. Chem. B 107 (2003) 8327.
[28] L.S. Du, A. Samoson, T. Tuherm, C.P. Grey, Chem. Mater. 12 (2000) 3611.
[29] C.P. Grey, D.R. Corbin, J. Phys. Chem. 99 (1995) 16821.
[30] Y. Xiao, M.S. thesis, SUNY-Stony Brook, 2001.
[31] K.H. Lim, C.P. Grey, Chem. Commun. 20 (1998) 2257.
[32] K.H. Lim, F. Jousse, S.M. Auerbach, C.P. Grey, J. Phys. Chem. B 105 (2001) 9918.
[33] J.A. Wang, X. Bokhimi, A. Morales, O. Novaro, T. Lopez, R. Gomez, J. Phys. Chem. B 103 (1999) 299.
[34] D.F. McMillan, D.M. Golden, Ann. Rev. Phys. Chem. 33 (1982) 493.
[35] T.P. Beebe, J.E. Crowell, J.T. Yates, J. Phys. Chem. 92 (1988) 1296.
[36] T. Krahl, R. Strosser, E. Kemnitz, G. Scholz, M. Feist, G. Silly, J.-Y. Buzare, Inorg. Chem. 42 (2003) 6474.